Influence of the Size Reduction on the Thermal Conductivity of Bismuth Nanowires

Ibrahim Nazem Qader[1] & Botan Jawdat Abdullah[2] & Muhammad Abdullah Hassan[1] & Peshawa H. Mahmood[3]

[1]Department of Physics, College of Science, Raparin University, Sulaimani, Iraq
[2]Department of Physics, College of Science, Salahaddin University, Erbil, Iraq
[3]Department of Chemistry, College of Science, Raparin University, Sulaimani, Iraq
Correspondence: Ibrahim Nazem Qader, Raparin University, Sulaimani, Iraq.
Email: ibrahimnazm@uor.edu.krd

Received: October 17, 2018 Accepted: December 15, 2018 Online Published: January 1, 2019

doi: 10.23918/eajse.v4i3sip55

Abstract: Theoretical calculations on the lattice thermal conductivity (LTC) of the bulk bismuth (Bi) and nanowires (NWs) have been studied with diameters 98 nm, 115 nm and 327 nm in the ⟨110⟩ direction from temperature range of 0 to 300 K. Several size dependent parameters are estimated to correlate the value of LTC using the modified Morelli-Callaway model, including mass density, Umklapp, normal, boundary impurity, dislocation, and phonon-electron scattering rate. In a particular range of temperature, their effects are varied on the bell-shaped LTC. In accordance, Grüneisen parameter has been calculated for each case and the obtained values fitted with the experimental data of LTC. The result indicates that the impact of increasing the surface area to volume ratio is satisfied on the LTC for some Bi NWs. At a specific temperature, the LTC drops with the reduction of size of NWs. The effects of the variation in size on LTC are calculated and the obtained results are in good agreement with the experimental data.

Keywords: Lattice Thermal Conductivity, Bismuth, Nanowires, Mass Density, Morelli-Callaway Model

1. Introduction

Since, the amount of heat generated and conducted in microchips and other miniature electrical devices is an important physical quantity, that has to be taken into account by engineers who select materials, then the lattice thermal conductivity (LTC) of nanowires (NWs) has been the subject of great interest in experimental studies of thermoelectric devices, particularly at the nanoscale level. Among the materials used, Bi has attracted significant attention, especially with rhombohedral crystal structure (Roh *et al.*, 2011) due to highly anisotropic Fermi surface (Cornelius *et al.*, 2005; Moore, Pettes, Zhou & Shi, 2009), small effective electron mass (Li *et al.*, 2007), high carrier mobility (Choi *et al.*, 2000), the low density and the long mean free path (Liu, Chien, Searson, & Yu-Zhang, 1998). Bi has been extensively studied because of its unique properties including quantum confinement effects (Wang *et al.*, 2001), anisotropic carrier transport properties (Lin, Cronin, Ying, Dresselhaus, & Heremans, 2000), thermal medical therapies, and magnetoresistance effect (Xu *et al.*, 2008; Yang, Liu, Chien, & Searson, 1999).

Several experimental and theoretical investigations have been performed to show the effects of

Grüneisen parameter, isotopes, impurities, and defects on the lattice thermal conductivity (LTC) of NWs (Abdullah, Omar, & Jiang, 2016; Mamand, Omar, & Muhammad, 2012). Recently, the effect of carrier concentration and other size dependent parameters on LTC of Si and Ge NWs has been studied, firstly by Abdullah (2010) and then for Si NWs by Morelli, Roh and Qader (Morelli, Heremans, & Slack, 2002; I. N. Qader, Abdullah, & Karim, 2017; I. N. Qader & Omar, 2017; Roh *et al.*, 2011). On the other hand, Kamatagi *et al.* (2009) have investigated the effect of acoustic phonon confinement in the range (2 < T < 100 K) TC of free standing-thin film (FSTF) structures. Also, the LTC for Wurtzite GaN NWs is calculated by Mamand *et al.* (2012) by applying mathematical calculation. Next, the thermal conductivity of Ge and Ge–Si core–shell NWs are experimentally studied by Wingert *et al.* (2011) and theoretically calculated after by Mamand and Omar (2014).

In the present work, the Morelli-Callaway model (Callaway, 1959) of LTC is used and correlated for Bi NWs in comparison to the reported experimental data. The size dependent mass density and the influence of various types of scattering processes on the LTC of Bi NWs are considered including the Umklapp (U-process), normal, phonon-impurity, phonon-electron, phonon-boundary, and phonon-dislocation scattering. The effects of different parameters such as mean free path, lattice parameters, melting point, Debye temperature and acoustic group velocity are also considered in the calculations.

2. Theoretical Method

2.1 Lattice Thermal Conductivity of Semiconductor Bulk

The theoretical model used was originally formulated by Callaway (1959). Holland (1963) extended Callaway's model and achieved better results. Nowadays, the most widely used model for studying LTC is an extension of the Callaway method, which is modified by Asen-Palmer, Bartkowski, Gmelin, and Cardona (1997). In this model, the total LTC can be expressed (Gupta & Trikha, 1978) as,

$$\kappa = \kappa_L + 2\kappa_T \tag{1}$$

where both κ_L and κ_T are lattice thermal conductivities relating to both the longitudinal and transverse phonons, respectively. Similarly, the conductivity for each longitudinal and transverse mode is divided into the following parts,

$$\kappa_L = \kappa_{L_1} + \kappa_{L_2} \tag{2}$$

$$\kappa_T = \kappa_{T_1} + \kappa_{T_2} \tag{3}$$

where the modes of each longitudinal and transverse phonon are denoted by the superscripts L and T, respectively. The terms of standard Debye-Callaway, κ_{L_1} and κ_{L_2} in Equation 2 is expressed as,

$$\kappa_{L_1} = \frac{1}{3} A_L T^3 \int_0^{\theta_D^L/T} \tau_c^L(x) J(x)\, dx \tag{4a}$$

$$\kappa_{L_2} = \frac{1}{3} A_L T^3 \left[\int_0^{\theta_D^L/T} \frac{\tau_c^L(x)}{\tau_N^L(x)} J(x)\, dx\right]^2 \left[\int_0^{\theta_D^L/T} \frac{\tau_c^L(x)}{\tau_N^L(x)\tau_R^L(x)} J(x)\, dx\right]^{-1} \tag{4b}$$

Likewise, the κ_{T_1} and κ_{T_2} in Equation 3 can be written as,

$$\kappa_{T_1} = \frac{1}{3} A_T T^3 \int_0^{\theta_D^T/T} \tau_c^T(x) J(x)\, dx \tag{5a}$$

$$\kappa_{T_2} = \frac{1}{3} A_T T^3 \left[\int_0^{\theta_D^T/T} \frac{\tau_c^T(x)}{\tau_N^T(x)} J(x)\, dx\right]^2 \left[\int_0^{\theta_D^T/T} \frac{\tau_c^T(x)}{\tau_N^T(x)\tau_R^T(x)} J(x)\, dx\right]^{-1} \tag{5b}$$

where, $A_{L(T)} = \left(\frac{k_B}{\hbar}\right)^3 \left(\frac{k_B}{(2\pi^2 v_{L(T)})}\right)$ and $J(x) = x^4 e^x (e^x - 1)^{-2}$, $x = \frac{\hbar\omega}{k_B T}$

where $\hbar$ is the reduced Planck's constant, k_B is the Boltzmann constant, τ_R is the sum of scattering processes, τ_N is the relaxation time of normal and τ_c is the combined phonon relaxation time. Also, $v_{L(T)}$ stands for longitudinal (transverse) acoustic phonon velocities, ω denotes the phonon angular frequency, θ_D refers to the Debye temperature. The combined phonon relaxation rate $\left(\tau_C^{L(T)}\right)^{-1}$ can be expressed as: $\left(\frac{1}{\tau_C^{L(T)}}\right) = \left(\frac{1}{\tau_N^{L(T)}}\right) + \left(\frac{1}{\tau_R^{L(T)}}\right)$

The acoustic group velocity $v_{L(T)}$, which is the wave packet moves uniformly with the speed of sound (Simon, 2013) that is for the $\langle 110 \rangle$ direction can be expressed as,

$$v_L(\langle 110 \rangle) = \sqrt{\frac{1}{2}\frac{C_{11} + C_{12} + 2C_{44}}{\rho}} \tag{6a}$$

$$v_T(\langle 110 \rangle) = \sqrt{\frac{C_{44}}{\rho}} \tag{6b}$$

where C_{11}, C_{12} and C_{44} are the elastic constants and ρ is the mass density. In terms of acoustic group velocity, the Debye temperature $\theta_D^{L(T)}$ for longitudinal and transverse acoustic branches can be estimated (Morelli *et al.*, 2002) as,

$$\theta_D^{L(T)} = \left(\frac{\omega_{L(T)}\pi^2}{V}\right)^{1/3} \frac{\hbar\, v_{L(T)}}{k_B} \tag{7}$$

where $\omega_{L(T)}$ represent the longitudinal (transverse) phonon frequency and V is the volume.

2.2 Phonon Scattering Rates

LTC of semiconductor crystal is affected by many resistive scattering processes. In this work, all resistive scattering processes that are limiting the thermal conductivity are $\boldsymbol{\tau_U^{L(T)}}$,$\boldsymbol{\tau_N^{L(T)}}$, $\boldsymbol{\tau_M^{L(T)}}$, $\boldsymbol{\tau_{ph-e}^{L(T)}}$, $\boldsymbol{\tau_B^{L(T)}}$ and $\boldsymbol{\tau_{DC}^{L(T)}}$. According to Matthiessen's rule (Holland, 1963), the total combined relaxation rate for both longitudinal and transverse modes can be expressed as,

$$\left(\frac{1}{\tau_C^{L(T)}}\right) = \left(\frac{1}{\tau_U^{L(T)}}\right) + \left(\frac{1}{\tau_N^{L(T)}}\right) + \left(\frac{1}{\tau_M^{L(T)}}\right) + \left(\frac{1}{\tau_B^{L(T)}}\right) + \left(\frac{1}{\tau_{ph-e}^{L(T)}}\right) + \left(\frac{1}{\tau_{DC}^{L(T)}}\right) \tag{8}$$

The relaxation rate by the Umklapp scattering rate is dominant at the temperature in the region of

$T \geq 0.1\theta_D$ (Lü, Chu & Shen, 2003). This may differ for different phonon modes due to the dependence of both transverse and longitudinal Debye temperature, phonon velocities and Grüneisen parameter. Thus, the Umklapp scattering rate for longitudinal and transverse phonons was given by Slack and Galginaitis (Morelli *et al.*, 2002) as,

$$\left[\tau_U^{L(T)}\right]^{-1} = B_U^{L(T)} \left(\frac{k_B}{\hbar}\right)^2 x^2 T^3 e^{-\left(\theta_D^{L(T)}/3T\right)} \quad (9)$$

with, $B_U^{L(T)} = \frac{\hbar \gamma_{L(T)}^2}{M\, v_{L(T)}^2 \theta_D^{L(T)}}$

where $B_U^{L(T)}$ is the Umklapp parameter strength, $\gamma_{L(T)}$ refers to the Grüneisen anharmonicity parameter and M is the average atomic mass. The Herring (1954) mechanism suggested that the appropriate form for the scattering rate due to phonon-phonon normal scattering (longitudinal or transverse) is given as,

$$\left[\tau_N^L\right]^{-1} = B_N^L \omega^2 T^3 \quad (10a)$$

where $B_N^L = \frac{k_B^3 v_L^2 V}{M\hbar^3 v_L^5}$ and

$$\left[\tau_N^T\right]^{-1} = B_N^T \omega T^4 \quad (10b)$$

and $B_N^T = \frac{k_B^4 v_T^2 V}{M\hbar^3 v_T^5}$ and $B_N^{L(T)}$ is a constant independent of ω and T.

As the phonons propagate through the crystal, they can be scattered by lattice imperfections such as point defects (isotope atoms and impurity) and dislocations, Klemens (1955) reported an expression for the relaxation rate for phonon scattering by point defect as:

$$\left[\tau_M^{L(T)}\right]^{-1} = \frac{V\,\Gamma}{4\pi\, v_{L(T)}^3}\omega^4 + \frac{3V^2S^2}{\hbar\, v_{L(T)}^3} N_{imp} \quad (11)$$

where S refers to the scattering factor and its value is close to unity (Klemens, 1955), N_{imp} is the impurity concentration and Γ is the measure of the strength of the mass difference scattering and defined as,

$$\Gamma = \sum_i f_i \left(1 - \frac{M_i}{\bar{M}}\right)^2 \quad (12)$$

where f_i is the fractional concentration of the impurity atoms of mass M_i, $\bar{M} = \sum_i f_i\, Mi$, where $\bar{M}$ is the average atomic mass and is equal to (208.98038 amu) for Bi. Regarding Bi isotopes are nearly 100% ^{209}Bi. Thus, according to the Equation 12, the value of f_i, and as well as Γ is found to be equal to zero.

On the other hand, the phonon-boundary scattering rate is assumed independent of temperature and frequency, and can be estimated from,

$$\left[\tau_b^{L(T)}(L)\right]^{-1} = \frac{v_{L(T)}}{d} \quad (13)$$

where d is the effective diameter of the sample. Phonons can be scattered by electrons. Hence, the phonon-electron scattering is a resistive process and it significantly influences the LTC of the NWs. The rate of the phonon-electron scattering is shown to be proportional to electron concentration density as follows,

$$\left[\tau_{ph-e}^{L(T)}(x)\right]^{-1} = \frac{n_e E^2 x}{\rho\, v_{L(T)}^2\, \hbar}\sqrt{\frac{\pi m^* v_{L(T)}^2}{2k_B T}} \times \exp\left(-\frac{m^* v_{L(T)}^2}{2k_B T}\right) \quad (14)$$

where n_e is the electron concentration density and E the deformation potential.

Furthermore, the presence of a crystal dislocation is another reason to scatter phonons. Nabarro (1951) separated the effects of the scattering of phonons on the core of the dislocation lines from the scattering of phonons by the elastic strain field within the dislocation lines. Scattering of phonons indicates that it has the short-range interaction at the core of dislocation lines, while it has a long-range interaction at the elastic strain field of dislocation lines. Similar to the three-phonon Umklapp processes (Nabarro, 1951), the phonon scattering rate can be used as,

$$\left[\tau_{DC}^{L(T)}(x)\right]^{-1} = \eta\, N_D \frac{V_o^{4/3}}{v_{L(T)}^2}\left(\frac{k_B T}{\hbar}\right)^3 x^3 \quad 15)$$

where N_D represents the number of dislocation lines per unit area and η is the weight factor. Where η illustrates the mutual tendency of dislocation lines and the direction of the temperature gradient. This value was found by integration $\eta = 0.55$ (Klemens, 1955).

2.3 Lattice Thermal Conductivity of Nanowires

2.3.1 Mean Bond Length

The mean bond length $\boldsymbol{d_{mean}}(\infty)$ is an average distance which a phonon covers in its wavelike pattern without any reflection or deflection for bulk state but at the nanoscale, its size dependent. The mean bond length for the nanoscale range $\boldsymbol{d_{mean}}(\boldsymbol{r})$ is inversely proportional with $\boldsymbol{r}$and reaches a peak at $\boldsymbol{r = r_c}$, which is denoted by $\boldsymbol{d_{mean}}(\boldsymbol{r_c})$ (Omar, 2012). The change of $\boldsymbol{d_{mean}}(\boldsymbol{r})$ as a function of $\boldsymbol{r}$is determined as,

$$\Delta d_{mean}(r) = \Delta d_{mean}(r_c)\left[\exp\left(\frac{-2(S_m(\infty) - R)}{3R\left(\frac{r}{r_c} - 1\right)}\right)\right]^{1/2} \quad (16)$$

where R is the ideal gas constant and S_m is the vibrational entropy while r_c denotes a critical radius at which all atoms of the particle are located on its surface and it is given by $r_c = [3 - D]h$, where h and $d_{mean}(r)$ (Omar, 2012) can be calculated as,

$$h = 1.429\, d_{mean}(\infty), \quad (17)$$

where,

$$d_{mean}(r) = h - \Delta d_{mean}(r), \quad (18)$$

where the bulk mean bond length is,

$$d_{mean}(\infty) = h - \Delta d_{mean}(r_c). \quad (19)$$

The value of the vibrational entropy is affected by the enthalpy of melting, $H_m(\infty)$ and the bulk melting temperature, $T_m(\infty)$. Therefore, its value given by the following relation,

$$S_m(\infty) = H_m(\infty)/T_m \quad (20)$$

where $H_m(\infty)$ as a function of bulk melting temperature can be written as,

$$H_m(\infty) = -10^{-5} T_m^2(\infty) + 0.059\, T_m(\infty) - 21.33 \quad (21)$$

2.3.2 Size Dependent Lattice Constant and Mass Density

The values of $a(r)$ are estimated as,

$$a(r) = \frac{4}{\sqrt{3}} d_{mean}(r) \quad (22)$$

and the size dependent volume $V(r)$ of the unit cell can be computed as follows,

$$V(r) = \left[\frac{a(r)}{2}\right]^3 \quad (23)$$

The theoretical size dependent volume $V(r)$ and mass density $\rho(r)$ of nanocrystalline materials were given by Abdullah, Jiang and Omar (2016) and can be expressed as,

$$\rho(r) = \rho(\infty) \frac{V(\infty)}{V(r)} \quad (24)$$

where $\rho(\infty)$ is the bulk mass density.

2.3.3 Size Dependent Melting Temperature

The melting point of a semiconductor material has a great effect on the material properties by the size and dimension of nanocrystals as well as the bulk overall melting entropy (Omar, 2012). The size dependent melting point $T_m(r)$ is expressed (Omar, 2012) as,

$$\frac{T_m(r)}{T_m(\infty)} = \left(\frac{V(r)}{V(\infty)}\right)^{2/3} \exp\left[-\frac{2(S_m(\infty) - R)}{3R\left(\frac{r}{r_c} - 1\right)}\right] \quad (25)$$

2.3.4 Size Dependent Debye Temperature and Phonon Group Velocity

Debye temperature is considered as one of the most important physical parameters that depends on the type and structure of the material. It is related to the vibrational frequency of the atoms in their crystalline lattice. Also, it is a separation line between classical and quantum mechanical behavior of phonons. Size-dependent Debye temperature $\theta_D^n(r)$ can be computed by using Lindmann's formula (Liang & Li, 2006):

$$\left(\frac{\theta_D^n}{\theta_D^B}\right)^2 = \frac{T_m^n}{T_m^B} \quad (26)$$

where the acoustic group velocity for isotropic systems can be related to a Debye temperature (Post, 1953) and can be expressed as,

$$\frac{v^n}{v^B} = \frac{\theta_D^n}{\theta_D^B} \quad (27)$$

3. Results and Discussion

Using the formalism described above, an analysis of the LTC is presented for both bulk and Bi NWs with diameter 98, 115 and 327 nm. All material parameters used for calculating LTC are listed in Table 1. Values of Bi elastic constants C_{11}, C_{12} and C_{44} which are used to calculate the longitudinal and transverse acoustic group velocity for growth direction ⟨110⟩ through equations 6a and 6b, respectively, are equal to 63.37 GPa, 24.49 GPa and 11.57 GPa (Madelung, 2012), respectively.

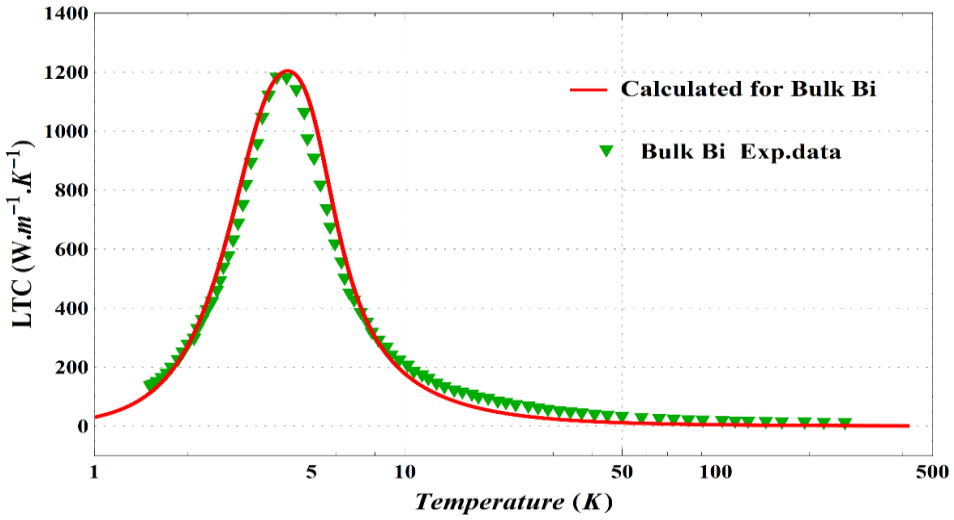

Figure 1: Calculated lattice thermal conductivity versus temperature from temperature range of 0 to 300 K of bulk Bi in comparison with the reported experimental data (Roh *et al.*, 2011).

Table 1: The material parameters for numerical calculation of LTC for bulk Bi

Ideal gas constant	R	8.314 JK^{-1} mol^{-1}	Ref.(Madelung, 2012)
First surface layer height	h	0.4078 nm	From Equation 17
Bulk overall melting entropy	$S_m(\infty)$	30 $JK^{-1}mol^{-1}$	From Equation 20
Average atomic mass		208.98038 amu	Ref.(Madelung, 2012)
Weight factor	η	0.55	Ref. (Caylor J, 2005)
Effective mass	m^*	0.113 m_e	Ref.(Madelung, 2012)

The LTC is computed through Equations 1 to 15 and the obtained size dependence values are tabulated in the Table 2 by using Equation 18 for mean path length, d_{mean}, Equation 22 for lattice parameter, a, Equation 23 for unit cell volume, V, Equation 24 for mass density, ρ, Equation 25 melting temperature, T_m, Equation 26 for longitudinal and transverse Debye temperature, $\theta_D^{L(T)}$ and Equation 27 for both longitudinal and transverse phonon group velocity, $v_{L(T)}$.

Table 2: Calculated size dependence values for the parameters of Bi NWs

r nm	d_{mean} Å	α Å	V $Å^3$	ρ $kg\,m^{-3}$	T_m K	θ_D^L K	θ_D^{T1} K	θ_D^{T2} K	v_L ms^{-1}	v_{T1} ms^{-1}	v_{T2} ms^{-1}
98	2.8626	6.6110	36.1171	9708	539.96	121.17	62.54	48.28	2345	1397	1077
115	2.8613	6.6079	36.0671	9722	540.63	121.43	62.62	48.34	2350	1398	1079
327	2.8564	6.5965	35.8814	9772	543.14	122.42	62.91	48.57	2369	1405	1084
Bulk	2.8537	6.5904	35.7813	9800	544.50	122.96	63.06	48.68	2380	1408	1087

In this work, some parameters are found as a fitting parameters, including impurity density, N_{imp}, surface roughness, ε, carrier concentration, n_e, Gruneisen parameter, γ, and lattice dislocation density, N_D, and their values are listed in Table 3.

Table 3: The fitted parameters of Bi NWs for calculating LTC at each diameter

r nm	N_{imp} m^{-3}	N_D m^{-2}	n_e m^{-3}	ε	L_c nm	L μm	γ_L	γ_T
98	9.0×10^{25}	6×10^{16}	2.5×10^{25}	0.002	98	5	0.012	0.011
115	8.0×10^{25}	5×10^{16}	2×10^{25}	0.001	115	5	0.011	0.010
327	3.0×10^{25}	1×10^{16}	1.18×10^{25}	0.0007	327	5	0.009	0.008
Bulk	5.0×10^{21}	9×10^{11}	3×10^{18}			300	6	0.7

The total LTC has been numerically calculated for both Bi bulk and NWs with diameter 98, 115 and 327 nm in the temperature range of 0 to 300 K as shown in the figures 1 and 2. The Figure 1 shows the temperature dependence of LTC of bulk bismuth. The Figure 2 illustrated the variation of LTC with diameter of NWs and there is a positive correlation between them. In addition, the dependence of LTC on temperature can be easily shown. It can be seen from the graph, as the temperature increases the LTC begins to increase. At low temperature, both the boundary and phonon-electron scattering rates have a remarkable effect on LTC. The LTC is highly dependent on temperature which is almost related to T^3. At moderate temperature, both the impurity and dislocation relaxation rates mostly affect the LTC of NWs, while at high temperature region, the most dominant scattering rate on LTC is Umklapp scattering.

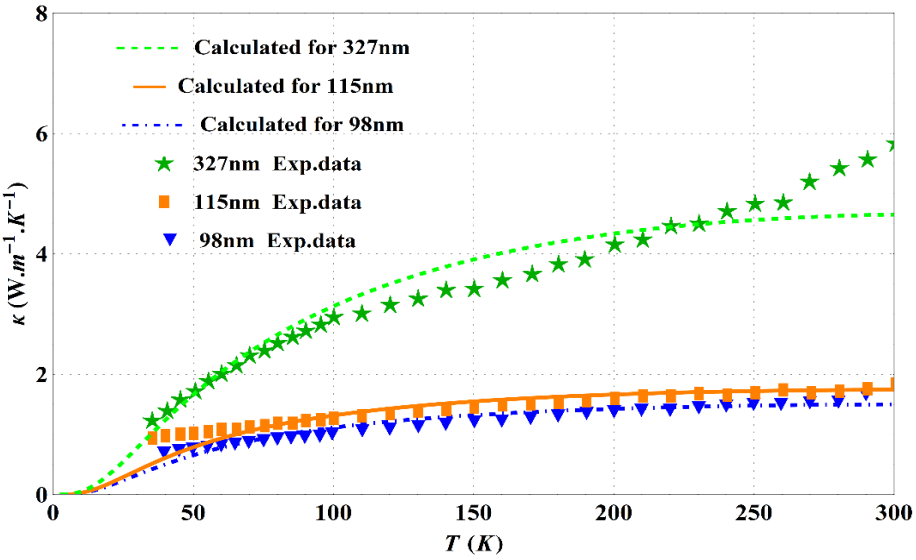

Figure 2: Calculated lattice thermal conductivity versus temperature for Bi NWs with diameters 98 nm, 115 nm and 327 nm from temperature range of 0 to 300 K in comparison with the reported experimental data (Roh *et al.*, 2011)

4. Conclusions

Experimentally, measuring some parameters is difficult or costly such as impurity, roughness or carrier concentration, then applying the theoretical model used in this work was quite sufficient to determine them. In this study, LTC was calculated for Bi bulk and nanowires of 98, 115 and 327 nm in diameter by applied Debye-Callaway model. Even though the LTC includes longitudinal and transverse group velocity and Debye temperature, whereas the transverse term again divided into two new terms due to Wurtzite Bi growth in the direction of ⟨110⟩. Since lattice parameter in the nanoscale is not constant, then it affects the quantitative values of several related parameters such as atomic volume, mass density. In addition, this influences on bond structure parameters like melting temperature, Debye temperature and group velocity. There are many novel equations handled to calculate these size dependent parameters. The results show that LTC for any particular temperature decreases with decreasing size of nanowires. Also, the model has a good correlation with experimental results. Some of those effects which cause these reduction in LTC are Umklapp scattering, normal scattering, boundary scattering, impurity density, dislocation, and carrier density

in the specimen.

Acknowledgement

This study is partially supported by Ishik University Research Center.

References

Abdullah, B. J. (2010). Effect of size on lattice thermal conductivity in Si and Ge nanowires from 2K to room temperatures. *Physics of Aero Dispersed Systems, 47*, 67-80.

Abdullah, B. J., Jiang, Q., & Omar, M. S. (2016). Effects of size on mass density and its influence on mechanical and thermal properties of ZrO2 nanoparticles in different structures. *Bulletin of Materials Science, 39*(5), 1295-1302.

Abdullah, B. J., Omar, M. S., & Jiang, Q. J. (2016). Grüneisen Parameter and Its Related Thermodynamic Parameters Dependence on Size of Si Nanoparticles. *ZANCO Journal of Pure and Applied Sciences, 28*(4), 126-132.

Asen-Palmer, M., Bartkowski, K., Gmelin, E., & Cardona, M. (1997). AP Zhernov, AV Inyushkin, A. Taldenkov, and VI Ozhogin, KM Itoh and EE Haller. *Phys. Rev. B, 56*, 9431-9447.

Callaway, J. (1959). Model for lattice thermal conductivity at low temperatures. *Physical Review, 113*(4), 1046.

Caylor J, C. K., Stuart J, Colpitts T, Venkatasubramanian R. (2005). Enhanced thermoelectric performance in PbTe-based superlattice structures from reduction of lattice thermal conductivity. *Applied Physics Letters, 87*.

Choi, S., Wang, K., Leung, M., Stupian, G., Presser, N., Morgan, B., . . . & Tueling, M. (2000). Fabrication of bismuth nanowires with a silver nanocrystal shadowmask. *Journal of Vacuum Science & Technology A: Vacuum, Surfaces, and Films, 18*(4), 1326-1328.

Cornelius, T., Brötz, J., Chtanko, N., Dobrev, D., Miehe, G., Neumann, R., & Molares, M. T. (2005). Controlled fabrication of poly-and single-crystalline bismuth nanowires. *Nanotechnology, 16*(5), S246.

Gupta, I., & Trikha, S. (1978). Lattice Thermal Conductivity of Solid Neon in the Temperature Range 0.5 to 10 K. *Physica Status Solidi (b), 88*(2), 815-818.

Herring, C. (1954). Role of low-energy phonons in thermal conduction. *Physical Review, 95*(4), 954.

Holland, M. (1963). Analysis of lattice thermal conductivity. *Physical Review, 132*(6), 2461.

Kamatagi, M., Vaidya, R., Sankeshwar, N., & Mulimani, B. (2009). Low-temperature lattice thermal conductivity in free-standing GaN thin films. *International Journal of Heat and Mass Transfer, 52*(11-12), 2885-2892.

Klemens, P. (1955). The scattering of low-frequency lattice waves by static imperfections. *Proceedings of the Physical Society Section A, 68*(12), 1113.

Li, L., Yang, Y., Fang, X., Kong, M., Li, G., & Zhang, L. (2007). Diameter-dependent electrical transport properties of bismuth nanowire arrays. *Solid State Communications, 141*(9), 492-496.

Liang, L., & Li, B. (2006). Size-dependent thermal conductivity of nanoscale semiconducting systems. *Physical Review B, 73*(15), 153303.

Lin, Y.-M., Cronin, S. B., Ying, J. Y., Dresselhaus, M., & Heremans, J. P. (2000). Transport properties of Bi nanowire arrays. *Applied Physics Letters, 76*(26), 3944-3946.

Liu, K., Chien, C., Searson, P., & Yu-Zhang, K. (1998). Structural and magneto-transport properties of electrodeposited bismuth nanowires. *Applied Physics Letters, 73*(10), 1436-1438.

Lü, X., Chu, J., & Shen, W. (2003). Modification of the lattice thermal conductivity in semiconductor rectangular nanowires. *Journal of Applied Physics, 93*(2), 1219-1229.

Madelung, O. (2012). *Semiconductors: Data handbook*. Springer Science & Business Media.

Mamand, S., & Omar, M. (2014). *Effect of Parameters on Lattice Thermal Conductivity in Germanium Nanowires.* Paper presented at the Advanced Materials Research.

Mamand, S., Omar, M., & Muhammad, A. (2012). Nanoscale size dependence parameters on lattice

thermal conductivity of Wurtzite GaN nanowires. *Materials Research Bulletin, 47*(5), 1264-1272.

Moore, A. L., Pettes, M. T., Zhou, F., & Shi, L. (2009). Thermal conductivity suppression in bismuth nanowires. *Journal of Applied Physics, 106*(3), 034310.

Morelli, D., Heremans, J., & Slack, G. (2002). Estimation of the isotope effect on the lattice thermal conductivity of group IV and group III-V semiconductors. *Physical Review B, 66*(19), 195304.

Nabarro, F. (1951). *The interaction of screw dislocations and sound waves.* Paper presented at the Proceedings of the Royal Society of London A: Mathematical, Physical and Engineering Sciences.

Omar, M. (2012). Models for mean bonding length, melting point and lattice thermal expansion of nanoparticle materials. *Materials Research Bulletin, 47*(11), 3518-3522.

Post, E. (1953). On the characteristic temperatures of single crystals and the dispersion of the "debye heat waves". *Canadian Journal of Physics, 31*(1), 112-119.

Qader, I. N., Abdullah, B. J., & Karim, H. H. (2017). Lattice Thermal Conductivity of Wurtzite Bulk and Zinc Blende CdSe Nanowires and Nanoplayer. *Eurasian Journal of Science & Engineering, 3*(1), 9-26.

Qader, I. N., & Omar, M. (2017). Carrier concentration effect and other structure-related parameters on lattice thermal conductivity of Si nanowires. *Bulletin of Materials Science, 40*(3), 599-607.

Roh, J. W., Hippalgaonkar, K., Ham, J. H., Chen, R., Li, M. Z., Ercius, P., . . . Lee, W. (2011). Observation of anisotropy in thermal conductivity of individual single-crystalline bismuth nanowires. *ACS Nano, 5*(5), 3954-3960.

Simon, S. H. (2013). *The Oxford solid state basics*. OUP Oxford.

Wang, X., Zhang, J., Shi, H., Wang, Y., Meng, G., Peng, X., . . . Fang, J. (2001). Fabrication and temperature dependence of the resistance of single-crystalline Bi nanowires. *Journal of Applied Physics, 89*(7), 3847-3851.

Wingert, M. C., Chen, Z. C., Dechaumphai, E., Moon, J., Kim, J.-H., Xiang, J., & Chen, R. (2011). Thermal conductivity of Ge and Ge–Si core–shell nanowires in the phonon confinement regime. *Nano Letters, 11*(12), 5507-5513.

Xu, Y., Ren, Z., Ren, W., Cao, G., Deng, K., & Zhong, Y. (2008). Magnetic-field-assisted solvothermal growth of single-crystalline bismuth nanowires. *Nanotechnology, 19*(11), 115602.

Yang, F., Liu, K., Chien, C., & Searson, P. (1999). Large magnetoresistance and finite-size effects in electrodeposited single-crystal Bi thin films. *Physical Review Letters, 82*(16), 3328.